Department of Veterans Affairs

Journal of Rehabilitation Research and Development Vol. 37 No. 3, May/June 2000
Pages 273–281

Design enhancement of a solid ankle-foot orthosis: Real-time contact pressures evaluation

Michael D. Nowak, ScD; Khamis S. Abu-Hasaballah, PhD; Paul S. Cooper, MD
Department of Orthopaedic Surgery, University of Connecticut Health Center, Farmington, CT 06030-6144; Department of Civil & Environmental Engineering, University of Hartford, West Hartford, CT 06117-1599

Abstract—The purpose of our study was to evaluate all contact pressures between the molded ankle-foot orthosis (MAFO) and the subject during activities of daily living. The MAFOs studied are used clinically to reduce plantar contact pressures associated with foot ulcers in adult neuropathic diabetic subjects, alleviating abnormal pressures by redistributing them to low-pressure plantar regions. While effective, MAFOs are often not used by the subject due to weight and comfort issues. An understanding of the contact pressures between the subject and the orthosis is a first step in improving basic MAFO design. Four nonimpaired, young adult males were tested in this study. A right-side MAFO was custom-molded and fitted for each subject by the same orthotist. Real-time pressures were obtained for the entire contact area using the F-Scan pressure measurement system. The data obtained demonstrated high contact pressures along the metatarsals of the foot, around the heel and ankle, and adjacent to the strap attachment sites. No contact pressures were noted along the posterior calf region during any of the activities performed. These data suggest the calf region would be a suitable site for material removal for weight reduction and increased comfort, especially in warm weather. In addition, these data may be useful to orthotists in improving the basic design and to researchers as a starting point for performing complex finite element analysis on the MAFO.

Address all correspondence and requests for reprints to: Dr. Khamis Abu-Hasaballah, Balance & Gait Enhancement Laboratory—Bldg. 6, Department of Neurology, University of Connecticut Health Center, Farmington, CT 06030-6144; email: khamis@nso.uchc.edu.

Key words: *ankle, ankle-foot orthosis, F-Scan, MAFO, pressure.*

INTRODUCTION

Diabetes is a major illness with high incidence of foot complications. The national commission on diabetes reported that 5 to 15 percent of persons with diabetes will ultimately require an amputation (1). In the United States, more than 54,000 diabetes-related amputations, a rate of 8.3 per 1000, are performed each year (2). The cost for these complications was estimated at approximately $1.9 billion in 1986, with an annual Medicare cost of $107–153 million for diabetic amputations (3). In 1991, the cost of diabetes care was estimated at $40 billion with about $2 billion for amputation costs. Most of this cost was directed at treatment of diabetic complications. This has prompted the U.S. Department of Health to set a goal for the year 2000 of a 40 percent reduction in amputation rates among persons with diabetes (4).

Approximately 70 percent of diabetics develop neuropathy within 5 years of diagnosis. After 5 years, the incidence increases to almost 100 percent. Foot pathology is the most common complication requiring hospitalization (5). The percent of hospital admissions for foot disorders has increased from 25 percent in the late 1960s to over 50 percent in the 1980s. Diabetic foot disorders

account for 16 percent of total diabetic admissions and 23 total diabetic hospitalization days (6). It has been shown that between 41 and 70 percent of diabetics with a lower limb amputation do not survive more than 5 years postoperatively. Historically, up to 30 percent of such amputations require a contralateral amputation within 3 years, with the rate increasing to 51 percent within 5 years of the initial procedure (7,8).

One of the most serious complications is neuropathic foot ulceration that, untreated, can lead to lower limb amputation. The main cause of foot ulceration in the adult neuropathic diabetic is thought to be the presence of abnormally high plantar pressures secondary to neuropathy (9–12). These pressures may be present as a result of compromised foot function, such as in hindfoot tendon disorders and diabetic Charcot foot (13).

Early preventive intervention, including education and the use of orthotics, splints, and casts, leads to successful treatment up to 90 percent of the time, thus reducing the volume of amputations. Increasing evidence suggests that diabetics can be successfully treated with molded ankle-foot orthoses (MAFOs), thus reducing time and morbidity associated with long-term total contact casting. MAFOs are used to correct ankle-foot biomechanical abnormalities and to relieve elevated plantar pressures by redistributing them to low weight-bearing areas. Recent clinical studies have indicated that, although effective (14,15), current MAFO designs have been noted to have poor compliance for long-term use in the management of hindfoot tendon disorders and Charcot foot (13). This is attributed to discomfort resulting from the MAFO's bulk and weight.

As a first step in improving its design, one needs to understand the interaction between the MAFO and the subject vis-à-vis contact pressures. The actual pressures of the entire contact regions, however, are unknown. The purpose of this study was to determine these pressures during activities of daily living (ADLs), such as normal walking (gait), chair rise, stair rise, and pivoting on the orthosis. Since a MAFO design based solely on gait might fail during other high-stress activities, contact pressures during various ADLs are examined for their possible variant loading patterns on the MAFO. If it proves to be adequate under the most stressful of these conditions, one may expect that the MAFO will be adequate for the less stressful ones. Knowledge of these contact pressures will shed light on the loading patterns experienced by the device during the ADLs tested and will assist in making MAFO design modifications.

METHODS

The entire MAFO-subject contact pressures were quantified during the following ADLs: walking, stair climbing, chair rise, and pivoting.

Subjects

Four nonimpaired male controls between the ages of 23 and 44 years and weighing 69–88 kg were tested in this study. The mean age, height, and weight (±SD) for all subjects were 33.8 (±9.5) years, 174.8 (±9.1) cm, and 79.5 (±8.5) kg, respectively. Right-side MAFOs of the same design as those for adult diabetics with ulcers due to various pathologic conditions such as the Charcot foot, flaccid foot, and hindfoot tendon disorders, were custom-molded and fitted for each subject by our orthotist (Altman Prosthetic & Brace, Glastonbury, CT).

MAFO Manufacture

The manufacturing process consisted of three steps: 1) creating the negative mold, where an impression of the foot and calf was taken; 2) generating the positive mold, and 3) generating and fitting the actual MAFO to the subject (**Figure 1**). The MAFO was custom fit by the orthotist to achieve subjective maximal function and comfort in the manner normally performed on persons with foot disorders.

Pressure Measurements

Real-time contact pressures were obtained for the entire MAFO-subject interaction surface using the F-Scan pressure measurement system (TEKSCAN, Boston, MA). The F-Scan system consists of two foot-shaped pads, each of which has 960 sensing elements (sensels) for the real-time recording of contact pressures. The pads can be hand-trimmed for a custom fit and have a density of 4 sensels per cm^2. Once calibrated, these pads give a reproducible characterization of real-time contact pressures (16–18).

Six new F-Scan sensors were used for each subject to cover all possible MAFO-subject contact zones. All were calibrated to 680 N (the weight one of the subjects) prior to trimming and testing. Four were then trimmed and shaped to the inner surface of the MAFO to minimize sensor wrinkling while maximizing coverage area; these were sufficient to cover all areas in the interior of the MAFO. They were arranged as follows: two in the calf shell region, one in the heel side/ankle region, and one in the plantar region. The first of the two remaining sensors

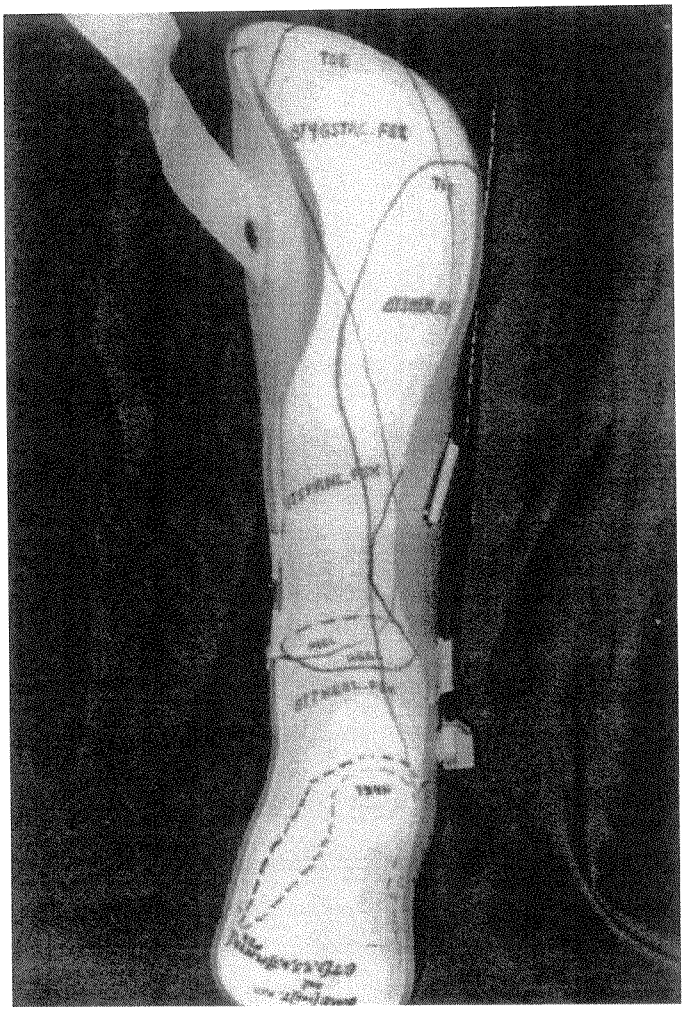

Figure 1.
A diagram of the molded ankle-foot orthosis (MAFO).

was positioned inside the shoe, at the MAFO-shoe interface, and the other underneath the calf shell strap. Since the F-Scan system allows two sensors to be recorded simultaneously, the MAFO-shoe interface sensor was used as a control for each test, with the other active channel shifted among the other sensors.

Pressure measurements were obtained during four different activities: walking, getting in and out of a chair, stair climbing, and pivoting over the MAFO. Before recording gait, the subject was instructed to walk at normal pace across the room (total distance 6 m) to precondition his walking timing. The chair rise was performed with the subject sitting fully on the chair (seat height = 48 cm, thickness = 3.8 cm, and soft seat and back cushions) and then rising upright. For stair climbing, the subject was instructed to step on a 35 cm high stool with a 25 cm diameter circular top. The right foot with the MAFO was the first to land on the stool and also the first to descend onto the floor. The subject was instructed to bring both feet to the stool top before starting to descend. In pivoting over the MAFO, the subject held his feet in a fixed position while rotating the upper torso.

The data were recorded at 20 frames per s, a rate experimentally determined to be the minimal frequency at which recording can be made without losing critical data. Each test was recorded for 30 s. This ensured that at least five readings were obtained during each test. After each test, and before the next recording, the data just recorded were displayed for visual inspection to insure integrity. If data proved to be corrupt (such as through sensor saturation or failure), the reading was discarded and the test repeated. The data were then stored for subsequent analysis on a PC with the F-Scan software. Average and peak pressure measures were obtained for this study.

F-Scan Sensor Temperature Characteristics

In an effort to study the temperature dependence of the F-Scan sensor, a static load was applied to a sensor sitting in a water bath at room temperature. After the sensor was let settle for 30 min, the bath temperature was slowly raised to 7°C above room temperature with numerous pressure measurements taken.

RESULTS

Pressure Measurements

To perform contact pressure measurements, six F-Scan sensors were placed on the MAFO, with two sensors being recorded simultaneously. To maintain consistency between runs, each test was performed five times, one run for each individual sensor, with that of the MAFO-shoe interface being recorded on the second channel as a control. Pressures from the control sensor were consistent across all trials for each subject, with a variability of ≤15 percent across all runs for any activity.

Average and peak contact pressures were obtained for the various activities tested. Schematics of typical average plantar pressures as a function of time obtained in this study are presented in **Figures 2–5.** It was noted that in certain regions of the MAFO the pressures were tangible (≤15 kPa) whereas in other areas they were minimal (≤15 kPa) or zero. Based on the anatomical divisions of the foot and ankle, the MAFO was divided into vari-

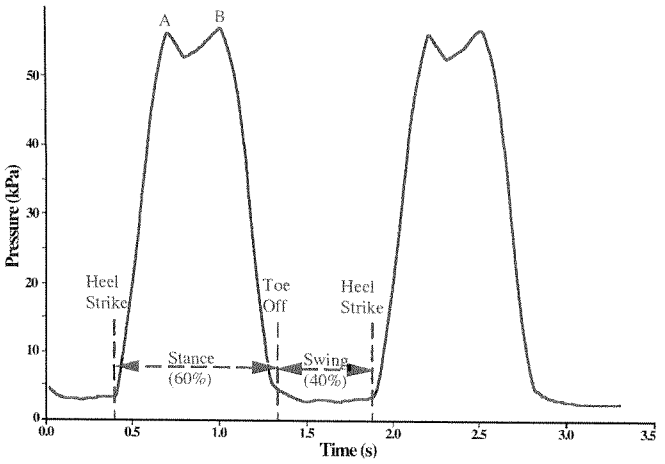

Figure 2.
Average plantar pressure as a function of time during gait.

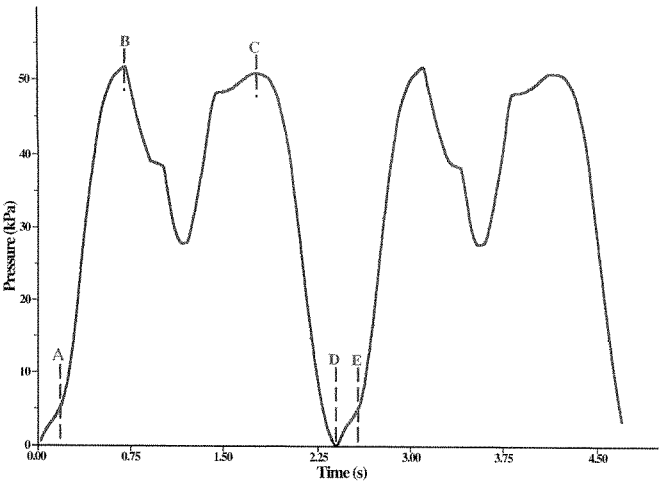

Figure 4.
Average plantar pressure as a function of time during stair rise.

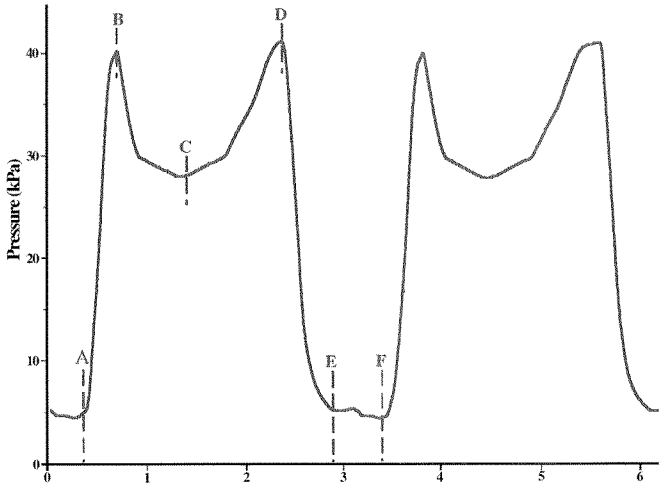

Figure 3.
Average plantar pressure as a function of time during chair rise.

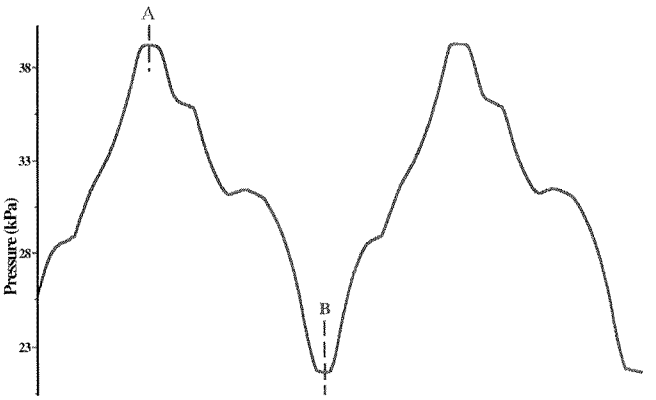

Figure 5.
Average plantar pressure as a function of time during pivoting on the MAFO.

ous regions as follows: inner MAFO plantar heel, inner MAFO plantar mid-foot, inner MAFO medial metatarsal heads, inner MAFO lateral metatarsal heads, ankle/side of heel, exterior MAFO plantar heel, exterior MAFO plantar mid-foot, exterior MAFO medial metatarsal heads, and exterior MAFO lateral metatarsal heads. In addition, regions in the calf shell that showed significant pressures were also mapped: the lateral calf shell flange, medial calf shell flange, and calf shell strap. These subdivisions are shown in **Figure 6.** The toe region of the foot was excluded since the MAFO did not encompass it and thus did not have any direct pressure effects.

Tables 1–4 present the average and peak contact pressures seen in the various MAFO regions during the different activities tested. In addition, **Table 5** presents strap forces during the instances when the strap was active. Since the pressure distribution during stair and chair rises was symmetrical (points C, **Figures 3** and **4**), data for these activities reported in **Tables 2** and **4** were taken at either point B or C.

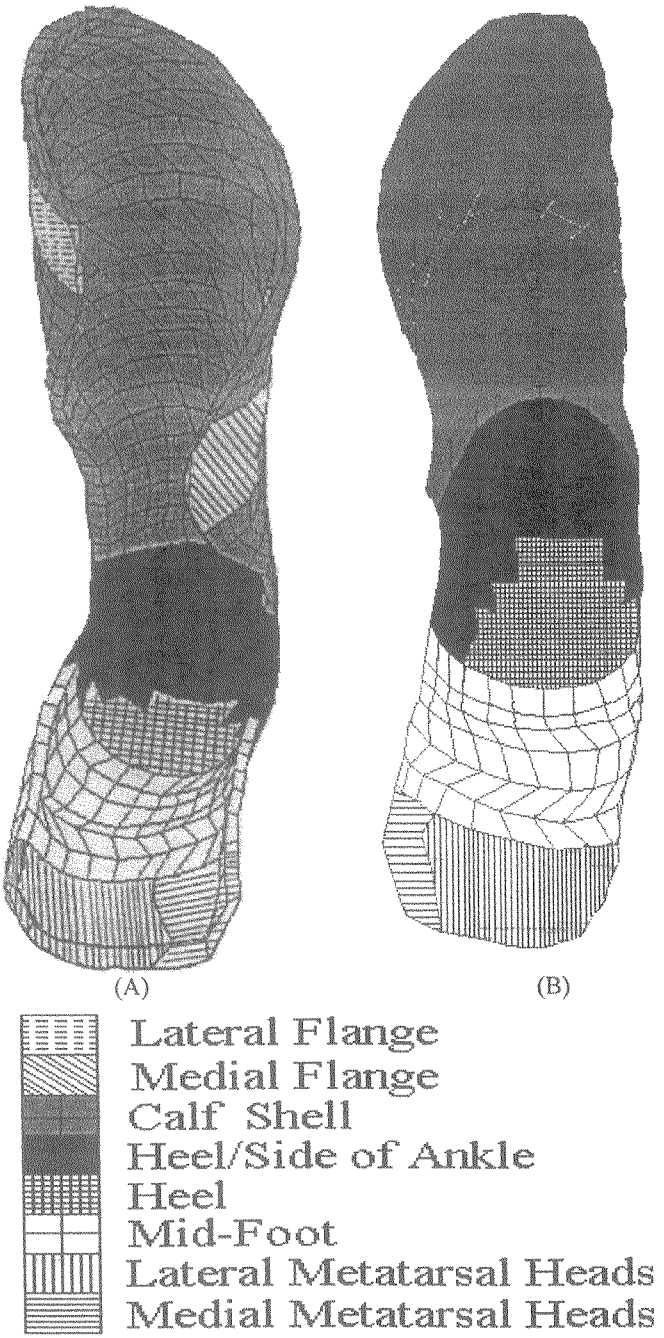

Figure 6.
Division of the MAFO into various inner (A) and outer (B) regions.

F-Scan Sensor Temperature Characteristics

In studying the temperature dependence of the F-Scan sensor, it was observed that sensor pressure reading was unchanged during the initial 4°C temperature rise. As the temperature was further raised, however, pressure readings drifted upward by 3 percent and 11.7 percent at 5 and 7°C above room temperature, respectively. Testing in our laboratory determined that the temperature inside the shoe did exceed 5°C after 10 min of walking at a normal pace.

DISCUSSION

This is the first study of its kind to identify pressures in the entire MAFO-subject contact regions during typical ADLs. The MAFOs utilized were based on those designed clinically for the diabetic neuropathic adult. The results of this study may provide better understanding of the MAFO-subject interaction and aid in the design of improved MAFOs.

Our study constitutes the first quantification of all MAFO-subject contact pressures. As can be seen in **Tables 1–4,** the pressures acting on the plantar exterior of the MAFO (at the MAFO-shoe interface) are substantially higher than in the MAFO interior (at the MAFO-subject interface). This demonstrates that the MAFO performs its designated function of decreasing plantar foot pressures. As an example, in the mid-stance phase of gait, the shoe exerts a pressure of 145 kPa on the exterior MAFO heel region, but the MAFO, in turn, exerts only 53.5 kPa on the plantar heel.

Overall, the average pressure distribution was noted to be homogenous during the various activities in the various regions. Most regions exhibited average pressures which ranged from 20 kPa (inner MAFO plantar mid-foot at heel-off) to 80 kPa (inner MAFO medial metatarsal heads in mid-stance). Gait testing demonstrated that the highest average and peak pressures were attained consistently in the different regions during the mid-stance phase (**Tables 1** and **3**). As the stance phase constitutes 60 percent of the gait cycle, it may be considered the most critical of all gait phases. Thus, when one is looking at maximal pressure limits exerted on the MAFO during gait, it might be sufficient to consider only the stance phase since all the other phases exhibit lesser pressures. By the same token, the swing phase may be the least important phase in terms of pressure distribution. As to the heel strike and heel-off phases, one is not able to make any classification and may only suggest that they are both more important than the swing phase but less critical than mid-stance.

During all the activities tested, the regions that most consistently underwent the pressures were the shoe insert and lower portion of the MAFO calf shell (the region

Table 1.
Average pressure (kPa) during gait.

Zone	Heel Strike	Mid-Stance	Heel-Off	Swing
Inner Plantar Heel	32.5±14.6	53.5±12.4	0	0
Inner Plantar Mid-Foot	23.5±3.1	39.7±14.2	15.3±10.7	0
Inner Medial Metatarsal	25.7±9.9	83.8±28.7	34.3±7.3	0
Inner Lateral Metatarsal	23.3±9.2	64.0±13.3	29.2±15.0	0
Ankle/Side of Heel	22.0±17.1	56.3±20.0	39.8±15.0	0
Lateral Shell Flange	0	11.3±2.5	0	0
Medial Shell Flange	0	35.8±20.3	0	0
Outer Plantar Heel	57.8±19.5	145.0±49.0	30.6±9.1	28.3±2.2
Outer Plantar Mid-Foot	44.0±10.4	119.5±28.6	41.6±9.7	39.5±7.2
Outer Medial Metatarsal	19.3±4.0	79.1±29.6	29.5±15.2	27.7±16.2
Outer Lateral Metatarsal	53.5±46.0	85.6±25.4	42.3±23.3	39.0±20.3

Table 2.
Average pressure (kPa) during chair rise, stair climbing, and pivoting on the MAFO.

Zone	Chair Rise	Stair Rise	Pivot
Inner Plantar Heel	45.5±17.0	63.8±35.3	50.8±23.4
Inner Plantar Mid-Foot	42.1±11.7	40.3±13.2	57.8±24.3
Inner Medial Metatarsal	46.5±6.2	55.9±13.5	52.3±18.3
Inner Lateral Metatarsal	39.4±24.8	33.5±12.0	29.2±17.1
Ankle/Side of Heel	50.3±15.4	65.3±16.8	27.5±7.4
Lateral Shell Flange	0	27.5±6.6	0
Medial Shell Flange	0	41.3±22.8	0
Outer Plantar Heel	99.6±51.5	95.5±40.0	105.0±48.9
Outer Plantar Mid-Foot	87.3±21.7	86.3±21.7	64.6±14.0
Outer Medial Metatarsal	38.0±19.0	30.8±8.8	38.8±38.4
Outer Lateral Metatarsal	40.5±21.1	48.8±18.7	40.5±12.5

Table 3.
Peak pressure (kPa) during gait.

Zone	Heel Strike	Mid-Stance	Heel-Off	Swing
Inner Plantar Heel	62.5±32.5	101.5±11.8	0	0
Inner Plantar Mid-Foot	47.5±17.9	101.9±39.8	30.0±20.1	0
Inner Medial Metatarsal	43.5±158.5	158.5±50.0	87.5±34.1	0
Inner Lateral Metatarsal	35.4±14.4	126.3±47.8	63.7±35.9	0
Ankle/Side of Heel	31.2±12.5	115±20.4	68.3±29.1	0
Lateral Shell Flange	0	20.1±10.2	0	0
Medial Shell Flange	0	84.5±21.9	0	0
Outer Plantar Heel	184.5±53.2	355.7±84.3	52.7±26.4	79.8±33.1
Outer Plantar Mid-Foot	170.8±79.2	576.3±206.0	143.5±55.9	133.0±45.8
Outer Medial Metatarsal	27.3±12.4	130.5±70.1	88.3±40.8	55.3±12.9
Outer Lateral Metatarsal	82.3±58.1	167.5±104.4	177.0±43.1	114.3±33.5

Table 4.
Peak pressure (kPa) during chair rise, stair climbing, and pivoting on the MAFO.

Zone	Chair Rise	Stair Rise	Pivot
Inner Plantar Heel	85.8±30.0	139.3±31.8	102.3±43.5
Inner Plantar Mid-Foot	104.5±4.4	104.5±23.3	114.3±53.7
Inner Medial Metatarsal	76.5±11.4	91.5±14.8	78.3±45.0
Inner Lateral Metatarsal	71.6±18.2	87.8±38.6	77.3±17.8
Ankle/Side of Heel	152.0±39.6	116.8±28.4	67.7±26.1
Lateral Shell Flange	0	33.3±13.2	0
Medial Shell Flange	0	89.0±25.7	0
Outer Plantar Heel	547.7±77.8	323.8±153.4	412.3±166.2
Outer Plantar Mid-Foot	374.0±82.6	328.0±97.9	219.0±46.0
Outer Medial Metatarsal	123.3±39.9	71.5±29.8	51.0±15.0
Outer Lateral Metatarsal	73.3±40.2	126.3±65.9	65.7±14.6

Table 5.
Strap forces (N) during the activities.

Gait: Heel-Off	Chair Rise	Stair Rise	Pivot
205.3±89.1	153.0±26.3	155.7±71.6	54.0±4.24

embracing the foot and ankles). The calf shell exhibited little or no pressure at all. Only in regions where the strap connects to the MAFO (lateral and medial calf shell flanges) did one see appreciable pressures during the mid-stance phase of gait and in stair climbing. This suggests that the MAFO calf shell would be a prime candidate for MAFO design modification through partial removal in order to reduce weight.

The strap was active during the heel-off phase of gait and in all the remaining activities tested. Thus, one may imply that the strap is more critical during these instances. One other note is the striking similarity of MAFO loading patterns while getting in and getting out of the chair.

Although studies examining and quantifying plantar foot contact pressures in different foot wear under various conditions are numerous, none have examined the contact pressures in an entire ankle-foot orthosis. The latter issue could perhaps be due to the technical difficulties encountered when attempting to instrument an entire MAFO surface. Few studies examined the MAFO-subject interaction in limited portions of the MAFO. For example, to obtain strains in the MAFO during walking and jumping, Chu (19) bonded six strain gages to the inner surface in the side heel/ankle of a polypropylene MAFO. Results indicated that the maximum deformation occurred in the lower lateral neck region of the MAFO. Novick et al. (15) examined the contact pressure under the first and third metatarsal heads, mid-foot, and heel in a rigid relief orthosis utilizing the Hercules and F-Scan pressure measurement systems. The Hercules system (Allegheny Ballistics Lab, Cumberland, MD) consisted of four capacitive pressure transducers 2 mm in thickness and 1.5 cm in diameter, and the F-Scan system consisted of a single trimmed sensor pad. Both systems recorded significant reductions in pressures in all regions examined with the brace. More recently, Grant et al. (20), constructed a simple, inexpensive device consisting of a 2.5 cm^2 single-cell sensor connected to a multimeter, to be used under the heel inside an orthosis. This device was used to determine the presence or absence of heel contact within the orthosis.

F-Scan Reliability and Accuracy

A number of studies have reported on the reliability of the F-Scan sensor. Koch et al. (16) showed that the intra-person coefficient of variation of a single sensor to be <23 percent. Furthermore, This intra-sensor variation was reduced to 15 percent by allowing a "warm-up" peri-

od of the sensor for about 5–10 min inside the shoe. Rose et al. (18) showed that pressure recordings from subsequent steps within a trial and also from the same sensors on the same patient on different days to be very similar. These reports are in agreement with a report by Mueller et al. (17), documenting good sensor reliability.

To understand reproducibility of the sensor, we loaded and evaluated F-Scan pads under two scenarios: 1) sine wave testing between 0 and 300 N at 0.1, 0.5, and 1.0 Hz, and 2) steady loading for 3 min at levels of 100, 150, 200, 300, 400, 500, and 600 N. For each test, the pads were calibrated to 300 N at 15 s after load application. Results showed that sensor data was reproducible for each test. Data drifted over time, but standard deviations were always within 10 percent of applied loading. Furthermore, the pads read forces above those actually applied after initial loading, with a steady value approximately 20 percent above true loading at 3 min. A chart based on these data was developed from which one can determine the true loading at any time during loading.

Initially, there was a question regarding the point in the experiment at which the sensors should be calibrated. This concern was raised as a result of a suggestion made by previous F-Scan users regarding the time- and temperature-dependence of the sensor. These users suggested that the sensor should be allowed a lengthy warm-up period prior to calibration and testing in order to cancel out these effects (17). In this study, however, it was not possible to calibrate the sensors after they had been fitted to the MAFO, because the process of trimming the sensors and then lining them on MAFO surface was laborious and time-consuming, and the subject was not expected to wait during this procedure. Rather, this process was completed prior to the testing; the subject was fitted with the instrumented MAFO soon after his arrival. In addition, the MAFO regions were of irregular shape and surface which would render sensor calibration at this point—after trimming and preparation inside the MAFO—difficult and unreliable. Therefore, all sensors were calibrated prior to trimming and use. The idea was to "correct" for any sensor time- and temperature-dependence once the measurements had been obtained. A correction factor would be obtained in our laboratory by testing the sensor under constant static loading at various times and temperatures in order to closely emulate actual testing conditions.

The manufacturer was contacted for feedback on sensor time and temperature characteristics. We were advised that those used previously were of the old generation and were time- and temperature-dependent. However, the generation of sensors used in this study was said to be free of these defects. This was confirmed in our laboratory whereby a sensor was statically loaded in a water bath for 30 min and then the bath temperature was steadily raised. Our results confirmed that the sensor measurements were unchanged after 30 min of constant loading at room temperature and changed slightly (3 percent) after a 5ºC rise. The sensor reading further changed to 11.7 percent after a 7ºC rise. To understand the implication of these changes on our data, the temperature inside a subject shoe was measured during gait: it was initially 2ºC above room temperature, increasing to 5ºC after 10 min of walking. Thus, one is confident that the data obtained in this study may be assumed to be time- and temperature-independent and no correction factor for these effects was needed. This is backed up by data from the MAFO-shoe interface control sensor that provided further evidence that the sensors were consistent throughout testing.

CONCLUSION

This is the first study to investigate the entire subject-MAFO pressure distribution in a clinically-based MAFO designed for neuropathic diabetic adults during ADLs such as walking, chair rise, stair rise, and pivoting on the MAFO. The majority of loading was seen in the shoe insert and lower calf shell regions of the MAFO, with limited pressures in the remainder of the calf shell. Maximal loading patterns in the MAFO were found to occur during the mid-stance phase of gait and stair climbing. This information may be useful to orthotists in improving basic MAFO design and to researchers as a starting point for performing complex finite element analysis on the MAFO.

ACKNOWLEDGMENTS

The authors would like to thank Mr. Ron Altman of Altman Prosthetics and Orthotics for providing the MAFOs used in this study.

REFERENCES

1. Most R, Sinnock P. Epidemiology of lower extremity amputation in diabetic individuals. Diabetes Care 1983;6:87–91.

2. National Institute of Diabetes and Digestive and Kidney Diseases. Ten agencies launch national campaign to reduce amputation rate. Washington DC; 1995. www.niddk.nih.gov/PressReleases/9November95PressRelease.html.
3. Federal Register—Congressional Record, Report #S2583-S2585; February 26, 1991.
4. Department of Health and Human Services. Health people 2000: national promotion and disease prevention objectives. Report No. DHH S9-50213, Government Printing Office, Washington DC; 1991.
5. Lie JT. The structure of the normal vascular system and its reactive changes. In: Juergens JL, Spittell JA, Fairbairn JF, editors. Peripheral vascular disease. Philadelphia: WB Saunders Company; 1988. p. 51–82.
6. Jacobs J, Sena M, Fox N. The cost of hospitalization for the leg complication of diabetes in the United States. Diabet Med 1990;8:528–9.
7. Leese B. The cost of diabetes and its complications. Soc Sci Med 1992;35(10):1303–10.
8. Mackey WC, McCullough JL, Colon TP, Shephard RD. The costs of surgery for limb-threatening ischemia. Surgery 1986;99(1):26–35.
9. Boulton AJM, Hardisty CA, Betts RP, et al. Dynamic foot pressure and other studies as diagnostic and management aids in diabetic neuropathy. Diabetes Care 1983;6:26–33.
10. Ctercteko GC, Dhanendran M, Hutton WC, Le Quesne LP. Vertical forces on the feet of diabetic patients with neuropathic ulceration. Br J Surg 1981;68:608–614.
11. Pollard JP, Le Quesne LP. Method of healing diabetic forefoot ulcers. Br Med J 1983;286:436–7.
12. Stokes IAF, Faris IB, Hutton WC. The neuropathic ulcer and the loads on the foot in diabetic patients. Act Orthop Scand 1975;46:839–47.
13. Lin SS, Lee TH, Wapner KL. Plantar ulcerations with equinus deformity of the ankle in diabetic patients: the effect of tendo-Achilles lengthening and total contact casting. Orthopedics 1996;19(5):465–75.
14. Moraros J, Hodge W. Orthotic survey preliminary results. J Am Podiatr Med Assoc 1993;83:139–48.
15. Novick A, Stone J, Birke JA, et al. Reduction of plantar pressures with the rigid relief orthosis. J Am Podiatr Med Assoc 1993;83(3):115–22.
16. Koch M. Measuring plantar pressure in conventional shoes with the TEKSCAN sensory system. Biomed Tech 1993;38(1):243–8.
17. Mueller MJ, Sinacore DR, Hoogstrate S, Daly L. Hip and ankle walking strategies: effects of plantar peak pressures and implication for neuropathic ulceration. Arch Phy Med Rehabil 1994;75:1196–200.
18. Rose NE, Feiwell LA, Ceacchiolo A. A method for measuring foot pressures using a high resolution, computerized insole sensor: the effect of heel wedges on plantar pressure distribution and center of force. Foot Ankle 1992;13(5):263–70.
19. Chu T. Experimental investigation: strain measurement on a polypropylene ankle-foot orthosis during normal gait. Adv Bioeng ASME:BED 1995;31:77–8.
20. Grant AD, Sala DA, Kummer JA, Kiriakatis A. A simple technique for assessing heel contact in orthoses. J Podiatr Orthop 1996;16(3):385–7.

Submitted for publication January 20, 1998. Accepted in revised form March 10, 1998.